Inorg. Chem. **2004**, *43*, 6774–6779

ZP8, a Neuronal Zinc Sensor with Improved Dynamic Range; Imaging Zinc in Hippocampal Slices with Two-Photon Microscopy

Christopher J. Chang,[†] Elizabeth M. Nolan,[†] Jacek Jaworski,[‡] Ken-Ichi Okamoto,[‡,§] Yasunori Hayashi,[‡,§] Morgan Sheng,[‡,§,||] and Stephen J. Lippard*[,†]

Department of Chemistry, Picower Center for Learning and Memory, RIKEN-MIT Neuroscience Research Center, and Howard Hughes Medical Institute, Massachusetts Institute of Technology, Cambridge, Massachusetts 02139

Received May 31, 2004

The synthesis of a difluorofluorescein monocarboxaldehyde platform and its use for preparing ZP8, a new member of the Zinpyr family of neuronal Zn^{2+} sensors, are described. By combining an aniline photoinduced electron transfer (PET) switch and an electron-withdrawing fluorescein scaffold, ZP8 displays reduced background fluorescence and improved dynamic range compared to previous ZP probes. The bright sensor undergoes an 11-fold increase in fluorescence intensity upon Zn^{2+} complexation ($\Phi = 0.03$–0.35) with high selectivity over cellular concentrations of Ca^{2+} and Mg^{2+}. In addition, sensors in the ZP family have been utilized for optical imaging in biological samples using two-photon microscopy (TPM). The cell-permeable ZP3 probe is capable of identifying natural pools of labile Zn^{2+} within the mossy fiber synapses of live hippocampal slices using TPM, establishing the application of this technique for monitoring endogenous Zn^{2+} stores.

Introduction

The neurophysiology of zinc is of emerging importance in human health and disease.[1,2] Histochemical studies reveal that the hippocampus, a region of the brain that controls learning and memory, accumulates up to 0.3 mM concentrations of loosely bound Zn^{2+} under normal conditions.[3,4] On the other hand, alterations in Zn^{2+} homeostasis are implicated in several neurological disorders;[4−6] abnormal patterns of ionic Zn^{2+} accumulation are found in patients with Alzheimer's disease,[7,8] epilepsy,[9] and traumatic head injury.[9]

Improved tools and tactics are needed to help elucidate the complex roles of labile Zn^{2+} in the brain and central nervous system. Optical imaging with two-photon microscopy (TPM) has facilitated the investigation of living systems with fluorescent reporters.[10,11] This technique is invaluable for studying calcium in neurobiology[12,13] and holds much promise for interrogating the neurochemistry of zinc. Whereas one-photon microscopy uses a single photon to excite a fluorophore into its excited state, TPM uses two photons of lower energy light to generate a fluorophore excited state. TPM has several advantages over standard one-photon excitation techniques, including reduced photodamage to living tissues and fluorophore, improved spatial resolution and sensitivity, and the ability to image thicker specimens.

Applying advances in optical imaging to study zinc neurophysiology requires the parallel development of Zn^{2+}-responsive fluorophores that operate in living systems.[2,14−16] To achieve this goal, several classes of small-molecule Zn^{2+} probes have been reported for use in cellular environments.[17−29]

* To whom correspondence should be addressed. E-mail: lippard@mit.edu.
† Department of Chemistry.
‡ Picower Center for Learning and Memory.
§ RIKEN-MIT Neuroscience Research Center.
|| Howard Hughes Medical Institute.

(1) Li, Y. V.; Hough, C. J.; Sarvey, J. M. *Science STKE* **2003**, pe19.
(2) Burdette, S. C.; Lippard, S. J. *Proc. Natl. Acad. Sci. U.S.A.* **2003**, *100*, 3605−3610.
(3) Frederickson, C. J. *Int. Rev. Neurobiol.* **1989**, *31*, 145−238.
(4) Frederickson, C. J.; Bush, A. I. *BioMetals* **2001**, *14*, 353−366.
(5) Bush, A. I. *Curr. Opin. Chem. Biol.* **2000**, *4*, 184−191.
(6) Cuajungco, M. P.; Lees, G. J. *Neurobiol. Dis.* **1997**, *4*, 137−169.
(7) Bush, A. I. *Trends Neurosci.* **2003**, *26*, 207−214.
(8) Suh, S. W.; Jensen, K. B.; Jensen, M. S.; Silva, D. S.; Kesslak, P. J.; Danscher, G.; Frederickson, C. J. *Brain Res.* **2000**, *852*, 274−278.
(9) Choi, D. W.; Koh, J. Y. *Annu. Rev. Neurosci.* **1998**, *21*, 347−375.
(10) Williams, R. M.; Zipfel, W. R.; Webb, W. W. *Curr. Opin. Chem. Biol.* **2001**, *5*, 603−608.
(11) Mainen, Z. F.; Maletic-Savatic, M.; Shi, S. H.; Hayashi, Y.; Malinow, R.; Svoboda, K. *Methods* **1999**, *18*, 231−239.
(12) Sabatini, B. L.; Oertner, T. G.; Svaboda, K. *Neuron* **2002**, *33*, 439−452.
(13) Brown, E. B.; Shear, J. B.; Adams, S. R.; Tsien, R. Y.; Webb, W. W. *Biophys. J.* **1999**, *76*, 489−499.
(14) Frederickson, C. J. *Science STKE* **2003**, pe18.
(15) Kikuchi, K.; Komatsu, K.; Nagano, T. *Curr. Opin. Chem. Biol.* **2004**, *8*, 182−191.
(16) Jiang, P.; Guo, Z. *Coord. Chem. Rev.* **2004**, *248*, 205−229.

10.1021/ic049293d CCC: $27.50
Published on Web 09/15/2004

Scheme 1

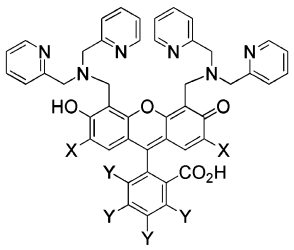

ZP1: X = Cl, Y = H
ZP2: X = H, Y = H
ZP3: X = F, Y = H
ZPF1: X = Cl, Y = F
ZPCl1: X = Cl, Y = Cl
ZPBr1: X = Cl, Y = Br
ZPF3: X = F, Y = F

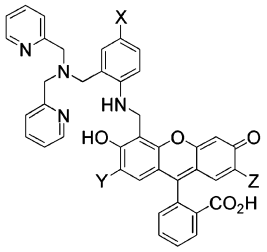

ZP4: X = H, Y = H, Z = Cl
ZP5: X = F, Y = H, Z = Cl
ZP6: X = Cl, Y = H, Z = Cl
ZP7: X = OMe, Y = H, Z = Cl
ZP8: X = H, Y = F, Z = F

We have devised the Zinpyr (ZP) family of Zn^{2+} sensors that give a positive fluorescence response upon Zn^{2+} coordination (Scheme 1).[30−35] These fluorescein-based reagents have high brightness values derived from sizable extinction coefficients and quantum yields, are selective for Zn^{2+} over cellular concentrations of Ca^{2+} and Mg^{2+}, and are available in cell-permeable and cell-impermeable forms. Previous work in our laboratory has established two different methods for controlling the pK_a values and attendant proton sensitivity of these photoinduced electron transfer (PET) sensors for neuronal Zn^{2+}: (i) introduction of electron-withdrawing groups on the fluorescein backbone,[34] and (ii) substitution of an aliphatic nitrogen PET switch by an aniline counterpart.[33] We reasoned that combining these two approaches would further improve the pH-dependent properties and dynamic range of the ZP probes. On the basis of this premise, we now report the synthesis and characterization of ZP8, an aniline-containing sensor based on a new monosubstituted difluorofluorescein platform. We also demonstrate the utility of ZP fluorophores for two-photon excitation experiments, including the first detection of endogenous Zn^{2+} pools using TPM.

Experimental Section

Materials and Synthetic Methods. Silica gel 60 (70−230 mesh, Merck) and octadecyl-functionalized silica gel (RP18, Aldrich) were used for column chromatography. Analytical thin-layer chromatography was performed using Merck 60 F254 silica gel and Merck RP-18 F254S silica gel (precoated sheets, 0.25 mm thick). Solvents for synthesis were of reagent grade or better and were dried according to standard methods.[36] 4-Fluororesorcinol[37] and 2-[bis-(2-pyridylmethyl)aminomethyl]aniline (**5**)[33] were synthesized according to published protocols. All other reagents for synthesis were purchased and used as received. ^{1}H NMR spectra were collected in $CDCl_3$ or CD_3OD at 25 °C at the MIT Department of Chemistry Instrumentation Facility (DCIF) on either a Varian Inova 500 or a Varian Mercury 300 spectrometer. All chemical shifts are reported in the standard δ notation of parts-per-million; positive chemical shifts are to higher frequency from the given reference. High-resolution mass spectral analyses were carried out at the MIT DCIF.

2-Methyl-4-fluororesorcinol (1). Under an argon atmosphere, 2-methylresorcinol (5.02 g, 40.4 mmol) was dissolved in dry acetonitrile (25 mL), and the solution was cooled to 0 °C. A solution of 1-chloromethyl-4-fluoro-1,4-diazabicyclo[2.2.2]octane bis(tetrafluoroborate) (15.0 g, 42.3 mmol) in dry acetonitrile (250 mL) was added dropwise to the cold resorcinol solution over a period of 1 h. The reaction was stirred at 0 °C for an additional 15 h under argon. The reaction was poured into ether (200 mL) and washed with saturated aq NaCl (3 × 300 mL). The organic layer was separated and dried over Na_2SO_4, and the solvent was removed by rotary evaporation. Flash column chromatography (silica gel, 4:1 hexanes/ethyl acetate) furnished resorcinol **1** as a beige powder (4.0 g, 71% yield). ^{1}H NMR ($CDCl_3$, 500 MHz): δ 6.79 (1 H, t, J = 9.0 Hz), 6.29 (1 H, m), 5.10 (1 H, d, J = 5.5 Hz), 4.13 (1 H, s) 2.17 (3 H, s). HRMS (ESI) calcd for $[M]^+$ 142.0425, found 142.0426.

2′-Carboxy-3-methyl-2,4-dihydroxy-5-fluorobenzophenone (2). Under an argon atmosphere, 2-methyl-4-fluororesorcinol (**1**, 1.20 g, 8.44 mmol) and phthalic anhydride (1.17 g, 7.90 mmol) were combined in dry nitrobenzene (30 mL). The mixture was cooled to 0 °C, and aluminum(III) chloride (2.45 g, 18.37 mmol) was added in one portion. The resulting dark olive slurry was allowed to warm to room temperature and stirred for an additional 16 h under argon. The reaction was poured into a vigorously stirring mixture of hexanes (360 mL) and 1 M HCl (150 mL). The precipitate was filtered and recrystallized twice from methanol/water to afford benzophenone **2** as an off-white powder (1.20 g, 49% yield). ^{1}H NMR (CD_3OD, 500 MHz): δ 8.11 (1 H, d, J = 7.5 Hz), 7.71 (1 H, t, J = 7.2 Hz), 7.64 (1 H, t, J = 7.5 Hz), 7.38 (1 H, d, J = 7.5 Hz), 6.54 (1 H, d, J = 10.5 Hz), 2.14 (3 H, s). HRMS (ESI) calcd for $[M - H]^-$ 289.0507, found 289.0502.

(17) Frederickson, C. J.; Kasarskis, E. J.; Ringo, D.; Frederickson, R. E. *J. Neurosci. Methods* **1987**, *20*, 91−103.
(18) Zalewski, P. D.; Millard, S. H.; Forbes, I. J.; Kapaniris, O.; Slavotinek, A.; Betts, W. H.; Ward, A. D.; Lincoln, S. F.; Mahadevan, I. *J. Histochem. Cytochem.* **1994**, *42*, 877−884.
(19) Hirano, T.; Kikuchi, K.; Urano, Y.; Nagano, T. *J. Am. Chem. Soc.* **2002**, *124*, 6555−6562.
(20) Maruyama, S.; Kikuchi, K.; Hirano, T.; Urano, Y.; Nagano, T. *J. Am. Chem. Soc.* **2002**, *124*, 10650−10651.
(21) Gee, K. R.; Zhou, Z.-L.; Qian, W.-J.; Kennedy, R. *J. Am. Chem. Soc.* **2002**, *124*, 776−778.
(22) Gee, K. R.; Zhou, Z. L.; Ton-That, D.; Sensi, S. L.; Weiss, J. H. *Cell Calcium* **2002**, *31*, 245−251.
(23) Sensi, S. L.; Ton-That, D.; Weiss, J. H.; Rothe, A.; Gee, K. R. *Cell Calcium* **2003**, *34*, 281−284.
(24) Lim, N. C.; Yao, L.; Freake, H. C.; Brückner, C. *Bioorg. Med. Chem. Lett.* **2003**, *13*, 2251−2254.
(25) Henary, M. M.; Fahrni, C. J. *J. Phys. Chem. A* **2002**, *106*, 5210−5220.
(26) Taki, M.; Wolford, J. L.; O'Halloran, T. V. *J. Am. Chem. Soc.* **2004**, *126*, 712−713.
(27) Kimura, E.; Aoki, S.; Kikuta, E.; Koike, T. *Proc. Natl. Acad. Sci. U.S.A.* **2003**, *100*, 3731−3736.
(28) Woodroofe, C. C.; Lippard, S. J. *J. Am. Chem. Soc.* **2003**, *125*, 11458−11459.
(29) Chang, C. J.; Jaworski, J.; Nolan, E. M.; Sheng, M.; Lippard, S. J. *Proc. Natl. Acad. Sci. U.S.A.* **2004**, *101*, 1129−1134.
(30) Walkup, G. K.; Burdette, S. C.; Lippard, S. J.; Tsien, R. Y. *J. Am. Chem Soc.* **2000**, *122*, 5644−5645.
(31) Burdette, S. C.; Walkup, G. K.; Spingler, B.; Tsien, R. Y.; Lippard, S. J. *J. Am. Chem. Soc.* **2001**, *123*, 7831−7841.
(32) Burdette, S. C.; Lippard, S. J. *Coord. Chem. Rev.* **2001**, *216−217*, 333−361.
(33) Burdette, S. C.; Frederickson, C. J.; Bu, W.; Lippard, S. J. *J. Am. Chem. Soc.* **2003**, *125*, 1778−1787.
(34) Chang, C. J.; Nolan, E. M.; Jaworski, J.; Burdette, S. C.; Sheng, M.; Lippard, S. J. *Chem. Biol.* **2004**, *11*, 203−210.
(35) Nolan, E. M.; Burdette, S. C.; Harvey, J. H.; Hilderbrand, S. A.; Lippard, S. J. *Inorg. Chem.* **2004**, *43*, 2624−2635.
(36) Pangborn, A. B.; Giardello, M. A.; Grubbs, R. H.; Rosen, R. K.; Timmers, F. J. *Organometallics* **1996**, *15*, 1518−1520.
(37) Yang, J.-J.; Su, D.; Vij, A.; Hubler, T. L.; Kirchmeier, R. L.; Shreeve, J. M. *Heteroat. Chem.* **1998**, *9*, 229−239.

4′-Methyl-2′,7′-difluorofluorescein Dibenzoate (3). Benzophenone **2** (3.50 g, 12.1 mmol) and 4-fluororesorcinol (1.55 g, 12.1 mmol) were ground together and melted into a liquid. Fused $ZnCl_2$ (2.00 g, 14.6 mmol) was added in three portions, and the temperature was increased to 250 °C. The reaction was cooled to room temperature and boiled in 300 mL of 1 N HCl. The amorphous material was separated. The remaining aqueous layer was extracted with dichloromethane (4 × 200 mL), and the organic phase was separated and taken to dryness. The resulting solid was combined with the amorphous material and dried under vacuum to afford a red-orange powder. Benzoic anhydride (12.0 g, 53.0 mmol) was added directly to the red-orange powder, and the mixture was refluxed in dry pyridine (80 mL) for 3.5 h under nitrogen. The reaction was cooled to 50 °C and poured into vigorously stirring water (400 mL). The precipitate was filtered and dried under vacuum to give crude **3** as an off-white powder that was used without further purification (4.82 g, 67% yield). HRMS (ESI) calcd for $[M]^+$ 590.1172, found 590.1162.

4′-Carboxaldehyde-2′,7′-difluorofluorescein (4). Crude 2′,7′-difluoro-4′-methylfluorescein dibenzoate (**3**, 2.60 g, 4.40 mmol) and 1,3-dibromo-5,5-dimethylhydantoin (1.26 g, 4.41 mmol) were combined in dry chlorobenzene (100 mL). Acetic acid (65 μL) and 1,1′-azobis(cyclohexanecarbonitrile) (VAZO 88, 60 mg, 0.245 mmol) were added, and the solution was stirred at 50 °C for 8 days. Hot water (100 mL) was added to the reaction, and the organic layer was separated, washed with water (2 × 100 mL), and dried over Na_2SO_4. The solvent was removed by rotary evaporation, and the remaining oil was dissolved in toluene (10 mL). Precipitation with ethanol (60 mL) gives the bromomethyl intermediate (2.2 g) that was used without further purification. A portion of this intermediate (200 mg, 0.30 mmol) and sodium bicarbonate (200 mg, 2.38 mmol) were combined in dry dimethyl sulfoxide (10 mL), and the mixture was heated under argon for 3 h at 150 °C. The reaction was cooled to 80 °C and poured into 4 N HCl (50 mL). The resulting precipitate was filtered and washed with water (3 × 25 mL). Purification by flash column chromatography (silica gel, 19:1 dichloromethane/methanol) yields aldehyde **4** as an orange solid (38 mg, 24% yield over two steps). ^{1}H NMR (CD_3OD, 500 MHz): δ 10.49 (1 H, s), 8.06 (1 H, d, J = 9.0 Hz), 7.93 (1 H, s), 7.57−7.62 (2 H, m), 7.19 (1 H, d, J = 9.0 Hz), 6.78 (1 H, d, J = 7.0 Hz), 6.64−6.75 (2 H, m). HRMS (ESI) calcd for $[M - H]^-$ 395.0362, found 395.0355.

4′-[2-{Bis(2-pyridylmethyl)aminomethyl}-*N*-methylaniline]-2′,7′-difluorofluorescein (Zinpyr 8, ZP8, 6). 4′-Carboxaldehyde-2′,7′-difluorofluorescein (**4**, 20 mg, 0.050 mmol) and 2-[bis(2-pyridylmethyl)aminomethyl]aniline (**5**, 16 mg, 0.053 mmol) were combined in a mixture of dry chloroform (2 mL) and dry methanol (2 mL). The wine-colored solution was stirred at room temperature for 24 h and diluted with dry 1,2-dichloroethane (3 mL). Sodium triacetoxyborohydride (22 mg, 0.104 mmol) was added in one portion, the solution color changed to pale orange, and the reaction was stirred for an additional 24 h at room temperature. Removal of the solvent and purification by preparative thin-layer chromatography (octadecyl-functionalized silica gel, methanol) afforded chemosensor **6** as an orange powder (24 mg, 70% yield). ^{1}H NMR (CD_3OD, 500 MHz): δ 8.28 (2 H, d, J = 5.0 Hz), 8.10 (1 H, d, J = 7.5 Hz), 7.70−7.77 (3 H, m), 7.44−7.50 (2 H, m), 7.33 (2 H, d, J = 7.5 Hz), 7.25 (1 H, d, J = 8.5 Hz), 7.10−7.14 (3 H, m), 7.02 (1 H, d, J = 7.5 Hz), 6.91 (1 H, d, J = 8.5 Hz), 6.78 (1 H, d, J = 7.5 Hz), 6.57−6.65 (1 H, m), 6.52 (1 H, d, J = 11.5 Hz), 4.53 (2 H, br s), 3.55−3.72 (6 H, m). HRMS (ESI) calcd for $[M - H]^-$ 683.2101, found 683.2114.

Spectroscopic Materials and Methods. Ultrol grade PIPES (piperazine-*N*,*N*′-bis(2-ethanesulfonic acid), Calbiochem), KCl (Alfa, Puratronic grade, 99.997%), and $ZnCl_2$ (Aldrich, 99.999%) were used as received. Millipore water was used for all aqueous solutions, which were filtered through 0.2 μm cellulose filters prior to use. All spectroscopic measurements were performed under simulated physiological conditions using buffer solutions containing 50 mM PIPES and 100 mM KCl adjusted to pH 7. A glass electrode (Orion), calibrated prior to each use, was used to determine solution pH. Solutions of Zn^{2+} were prepared from 100 mM stock solutions of $ZnCl_2$ in water. Absorption spectra were recorded on a Hewlett-Packard 8453A diode array spectrophotometer, and fluorescence spectra on a Photon Technology International (PTI) Quanta Master 4 L-format scanning spectrofluorometer equipped with an LPS-220B 75-watt xenon lamp and power supply, A-1010B lamp housing with integrated igniter, switchable 814 photon-counting/analogue photomultiplier detection unit, and MD-5020 motor driver. Samples for absorption and emission measurements were contained in 1 cm × 1 cm quartz cuvettes (3.5 mL volume, Starna). The experiments for measuring quantum yields, apparent dissociation constants (K_d), and metal ion selectivities were performed by using standard protocols.[31,34,35] Quantum yields were determined by reference to fluorescein in 0.1 N NaOH (Φ = 0.95).[38]

Preparation and Staining of Acute Mouse Hippocampal Slices. The whole brains of 60-day-old adult mice were removed. The hippocampi were dissected, cut into 400 μm-thick slices, and washed twice with Zn^{2+}-free Krebs ringer buffer; this medium was prepared according to a published method.[39] Slices were incubated with ZP8 or ZP3 (10 μM) for 20 min at 37 °C under 5% CO_2. Slices were then washed twice with Zn^{2+}-free Krebs ringer buffer and transferred to glass-bottomed dishes (MatTek) for imaging. Slices were imaged with a custom-made two-photon laser-scanning microscope based on an Olympus Fluoview 300 and BX50WI equipped with a 10× or 40× objective lens and 570 nm short pass emission filter, and a Spectraphysics Tsunami Ti:sapphire laser pumped by Millennia Xs. During imaging, slice samples were kept at 37 °C under 5% CO_2.

Results and Discussion

Synthesis of ZP8. The synthetic strategy for preparing ZP8 is outlined in Scheme 2. This convergent approach features a new fluorinated fluorescein monoaldehyde platform for attachment to a wide variety of metal ion receptors. Electrophilic fluorination of 2-methylresorcinol with 1-chloromethyl-4-fluoro-1,4-diazabicyclo[2.2.2]octane bis(tetrafluoroborate) affords 2-methyl-4-fluororesorcinol **1** in 71% yield after purification by column chromatography. Reaction of resorcinol **1** with phthalic anhydride in the presence of $AlCl_3$ generates 2′-carboxy-3-methyl-2,4-dihydroxy-5-fluorobenzophenone **2** in 49% yield after recrystallization from methanol/water mixtures. Condensation of benzophenone **2** and 4-fluororesorcinol with $ZnCl_2$ followed by the addition of benzoate protecting groups delivers crude 4′-methyl-2′,7′-difluorofluorescein dibenzoate **3** in 67% yield. ^{1}H NMR analysis indicated a ca. 2:1 mixture of the desired monomethyl compound and dimethyl side product.[35] Exhaustive attempts to purify product **3** were unsuccessful, and the crude

(38) Brannon, J. H.; Magde, D. *J. Phys. Chem.* **1978**, *82*, 705−709.
(39) Qian, W.-J.; Gee, K. R.; Kennedy, R. T. *Anal. Chem.* **2003**, *75*, 3468−3475.

Scheme 2

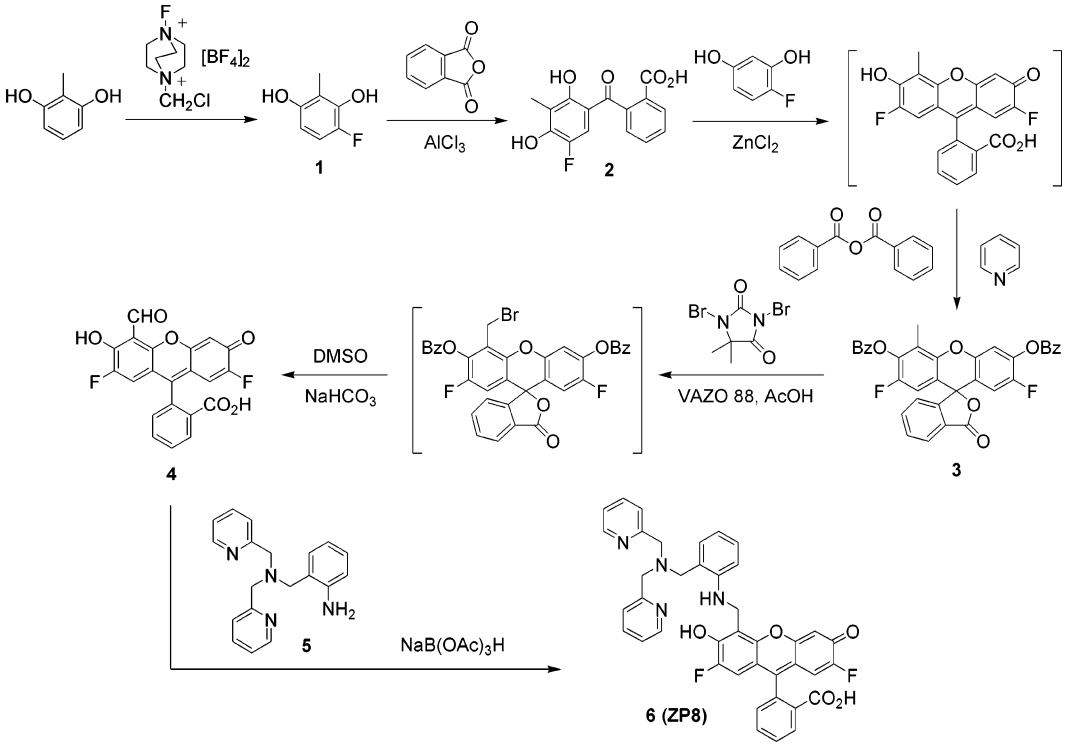

product was carried on without further purification to the next step. The crude fluorescein was brominated under mild free radical conditions and then oxidized to furnish aldehyde **4** in modest yield (24%) after column chromatography. The preassembled difluorofluorescein aldehyde is a useful synthon for the preparation of new sensor candidates. Schiff-base condensation of **4** and aniline **5** followed by reduction of the imine intermediate with sodium triacetoxyborohydride afforded ZP8 (**6**) in 70% yield.

Spectroscopic Properties and Optical Responses to Zn^{2+}. ZP8 was evaluated at physiological ionic strength and pH [50 mM PIPES (piperazine-*N*,*N*′-bis(2-ethanesulfonic acid)), 100 mM KCl, pH 7] in the presence of EDTA (ethylenediaminetetraacetic acid) to scavenge adventitious metal ions. Like other members of the ZP family,[34,35] the optical properties of ZP8 are dominated by the fluorescein chromophore, Table 1. In the absence of Zn^{2+}, the fluorinated sensor has an absorption maximum centered at 500 nm ($\epsilon = 8.1 \times 10^4$ M^{-1} cm^{-1}) with a corresponding emission maximum at 516 nm. ZP8 exhibits a weak fluorescence in its apo form ($\Phi = 0.03$) owing to the low pK_a value of 6.5 for its PET aniline nitrogen atom. Upon the addition of up to 1 equiv of Zn^{2+}, the fluorescence intensity of ZP8 increases by 11-fold ($\Phi = 0.35$, Figure 1), with a concomitant shift for both its absorption (489 nm, $\epsilon = 7.8 \times 10^4$ M^{-1} cm^{-1}) and emission (510 nm) maxima. The hypsochromic shift of the excitation peak for ZP8 upon Zn^{2+} binding indicates coordination of the fluorescein phenol oxygen atom, which perturbs the electronic structure of the fluorophore π system.[31] The structure most likely resembles the distorted octahedral geometry previously determined by X-ray crystallography for a 1:1 Zn^{2+} complex of a salicylaldehyde-derived binding model for the ZP4−ZP8 series.[33] The dynamic range

Table 1. Spectroscopic and Thermodynamic Data for the ZP Family[a,b]

	excitation (λ/nm, $\epsilon/\times 10^4$ M^{-1} cm^{-1})		emission (λ/nm, Φ)[c]			
	unbound	Zn^{2+}	unbound	Zn^{2+}	pK_a[d]	K_d/nM
ZP1[e]	515, 6.7	507, 7.8	531, 0.38	527, 0.87	8.4	0.7
ZP2	498, 4.4	490, 5.3	522, 0.25	517, 0.92	9.4	0.5
ZP3	502, 7.5	492, 8.5	521, 0.15	516, 0.92	6.8	0.7
ZP4	506, 6.1	495, 6.7	521, 0.06	515, 0.34	7.2	0.65
ZP5	504, 8.3	495, 9.1	520, 0.29	517, 0.48	9.6	0.5
ZP6	506, 8.9	495, 9.8	519, 0.10	517, 0.34	6.3	0.5
ZP7	505, 6.8	495, 7.7	521, 0.04	517, 0.05	6.9	0.5
ZP8	500, 8.1	489, 7.8	516, 0.03	510, 0.35	6.5	0.6
ZPF1	533, 9.9	525, 12.0	547, 0.11	544, 0.55	6.9	0.9
ZPCl1	534, 9.7	527, 12.0	550, 0.22	549, 0.50	7.0	1.1
ZPBr1	534, 4.5	528, 8.6	549, 0.25	547, 0.36	7.3	0.9
ZPF3	520, 8.7	510, 9.3	537, 0.14	533, 0.60	6.7	0.8

[a] All spectroscopic measurements were performed using 50 mM PIPES (piperazine-*N*,*N*′-bis(2-ethanesulfonic acid)), 100 mM KCl buffer, pH 7. [b] Data for ZP1 and ZP2 collected from ref 31, data for ZP3, ZPF1, ZPCl1, ZPBr1, and ZPF3 collected from ref 34, and data for ZP4−ZP7 collected from ref 35. [c] Reported quantum yields are based on fluorescein, $\Phi = 0.95$ in 0.1 N NaOH (ref 38). [d] Represents the pK_a value of the tertiary or aniline nitrogen responsible for PET switching in the Zn^{2+}-responsive ZP probes. [e] See Scheme 1 for nomenclature.

of ZP8 represents a ca. 2-fold improvement in fluorescence quantum yield response to Zn^{2+} compared to second-generation derivatives ZP3 and ZP4.[34,35]

The fluorescence response of ZP8 is Zn^{2+} selective. Figure 2 displays the fluorescence responses of a 1 μM solution of ZP8 in the presence of various divalent metal ions. ZP8 exhibits a selectivity profile similar to those of ZP4−ZP7.[35] The emission profiles of apo or Zn^{2+}-bound ZP8 are unperturbed in the presence of 2 mM Ca^{2+} or Mg^{2+}, indicating excellent selectivities for Zn^{2+} over these biologically competing alkaline earth cations. Other first-row transition metal ions including Cu^{2+}, Ni^{2+}, Co^{2+}, Fe^{2+}, and Mn^{2+} at 50-fold excess over probe produce no discernible

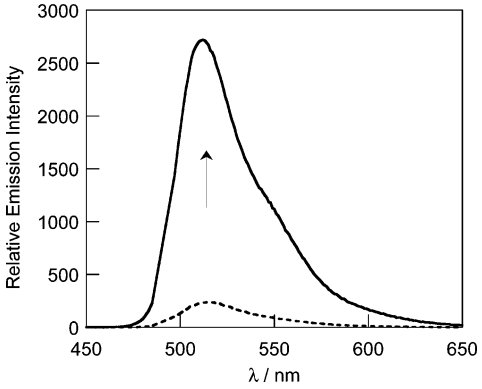

Figure 1. Fluorescence spectroscopic response of 1 μM ZP8 to a 10-fold excess of Zn^{2+}. The dotted and solid line spectra were recorded before and after Zn^{2+} addition, respectively. Spectra were acquired in 50 mM PIPES, 100 mM KCl, pH 7. Excitation was provided at 492 nm.

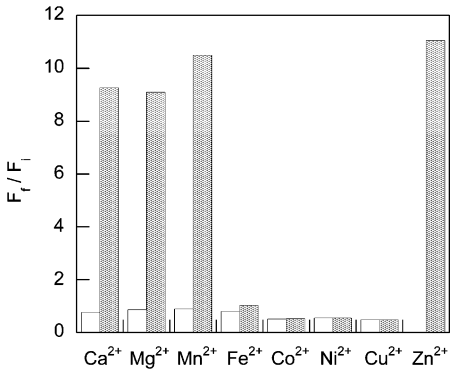

Figure 2. Fluorescence spectroscopic responses of ZP8 to various metal ions. Bars represent the final integrated fluorescence response (F_f) over the initial integrated emission (F_i). Spectra were acquired in 50 mM PIPES, 100 mM KCl, pH 7. White bars represent the addition of an excess of the appropriate metal ion (2 mM for Ca^{2+} and Mg^{2+}, 50 μM for all other metal ions) to a 1 μM solution of ZP8. Grey bars represent the subsequent addition of 50 μM Zn^{2+} to the solution. Excitation was provided at 492 nm, and the emission was integrated between 500 and 650 nm.

change in emission intensities. Of these transition metal ions, only the sample containing Mn^{2+} affords a positive fluorescence response upon subsequent addition of 50 μM Zn^{2+}. Although the other first-row transition metal ions compete with Zn^{2+} for the DPA chelator, the combination of selective fluorescence enhancement with Zn^{2+} and the greater availability of labile neuronal Zn^{2+} in vivo over these ions render ZP8 valuable for biological applications. The design of small molecule probes for specifically sensing Zn^{2+} over other metal ions remains a significant challenge for future synthetic chemistry.

The binding affinity of ZP8 for Zn^{2+} was characterized by using the standard dual-metal single-ligand buffer system.[30] Varying the total Zn^{2+} concentrations between 0 and 1 mM in the presence of constant concentrations of Ca^{2+} (2 mM) and EDTA (1 mM) delivers controlled concentrations of buffered free Zn^{2+} between 0 and 25 nM. ZP8 responds to nanomolar concentrations of free ionic Zn^{2+}. Titrations were performed in triplicate using different preparations of Ca^{2+}/Zn^{2+}/EDTA buffers to determine an apparent K_d value of 0.6 $\pm$ 0.1 nM for the fluorescence-responsive 1:1 Zn^{2+}−ZP8 complex (Figure 3).

Fluorescence Detection of Zn^{2+} in Live Hippocampal Slices Using Two-Photon Microscopy. We next sought to

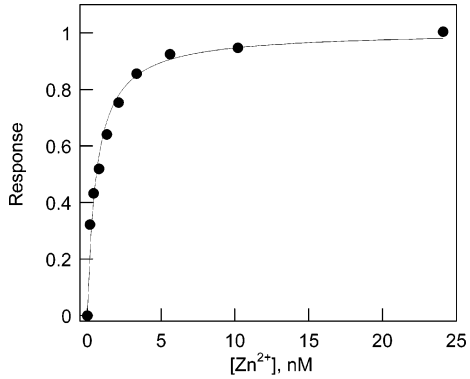

Figure 3. Normalized fluorescence spectroscopic response of 1 μM ZP8 to buffered Zn^{2+} solutions for K_d value determination. Data were acquired in 50 mM PIPES, 100 mM KCl, pH 7. Excitation was provided at 492 nm. The points shown are for free Zn^{2+} buffered at 0, 0.17, 0.42, 0.79, 1.3, 2.1, 3.4, 5.6, 10.2, and 24.1 nM, respectively.

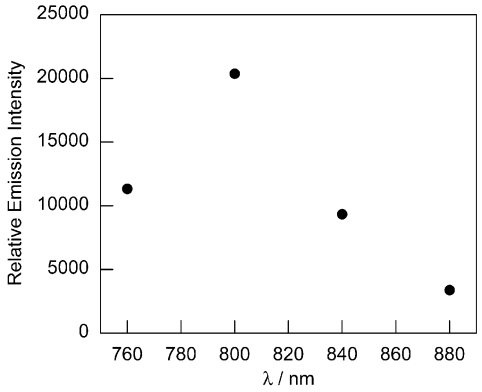

Figure 4. Relative fluorescence responses of Zn^{2+}-bound ZP3 upon two-photon excitation at 760, 800, 840, or 880 nm. Solutions contained 10 μM ZP3 and 200 μM Zn^{2+} in Krebs ringer buffer.

apply ZP8 and related ZP probes to image endogenous Zn^{2+} in biological samples with TPM. The ability of ZP8 to undergo two-photon excitation was evaluated under physiological conditions (Krebs ringer buffer). Solutions containing 10 μM ZP8 and 200 μM Zn^{2+} were excited in the range 760−880 nm; the highest fluorescence response for Zn^{2+}-bound ZP8 was with 760-nm excitation (data not shown). Subsequent experiments established that ZP8 is impermeable to cell membranes, as observed for the other aniline-containing members of the ZP series. We then turned our attention to ZP3, a cell-permeable probe that is capable of imaging endogenous pools of labile Zn^{2+} in live hippocampal neurons and slices using conventional one-photon confocal microscopy.[34] Solutions containing 10 μM ZP3 and 200 μM Zn^{2+} were excited in the range 760−880 nm (Figure 4); the highest fluorescence response for Zn^{2+}-bound ZP3 was with 800-nm excitation. Next, acute hippocampal slices from adult mice were incubated with 10 μM ZP3 for 20 min at 37 °C. Figure 5a displays the confocal TPM fluorescence image of a slice of an entire mouse hippocampus section produced by two-photon excitation at 800 nm. The slices are viable throughout the imaging experiments as determined by brightfield microscopy. As observed for slices imaged using one-photon excitation,[34] intense fluorescence staining is seen in the hilus of the dentate gyrus and the stratum lucidum of the CA3 region. Figures 5b and 5c display images taken at

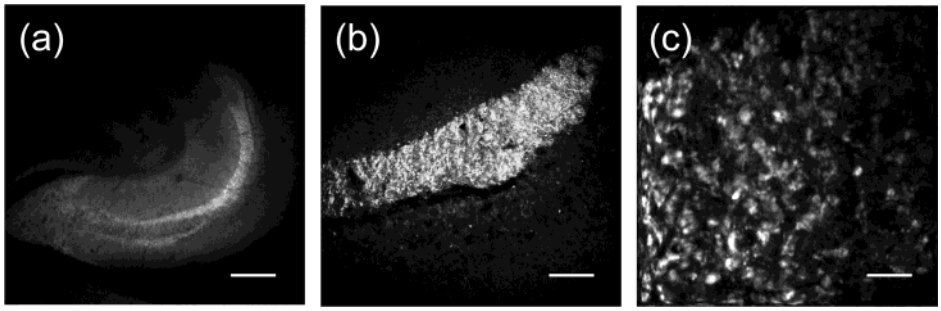

Figure 5. Confocal two-photon microscopy (TPM) of an acute mouse hippocampal slice stained with ZP3. Slices were incubated with 10 μM ZP3 for 20 min at 37 °C. Fluorescent images were produced upon excitation at 800 nm. (a) Magnification at 10× shows an entire slice section of a mouse hippocampus with all of the different zinc-containing cytoarchitectonic regions; scale bar = 200 μm. (b) Magnification at 40× highlights the stratum lucidum layer; scale bar = 50 μm. (c) Magnification at 200× captures and resolves individual giant mossy fiber boutons; scale bar = 10 μm.

higher magnifications that resolve the stratum lucidum layer and individual giant mossy fiber boutons, respectively. These experiments demonstrate that the ZP family undergoes effective two-photon excitation and that ZP3 is capable of imaging endogenous stores of labile Zn^{2+} in live biological samples using TPM.

Concluding Remarks

We have described the synthesis and characterization of ZP8, a new fluorescent Zn^{2+} sensor of the ZP family. This probe exhibits improved dynamic range compared to other members of the ZP series by combining an aniline PET switch with electronegative fluorophore substitution. ZP8 features an 11-fold fluorescence increase in response to Zn^{2+}, visible excitation and emission profiles, high brightness values, selectivity over cellular concentrations of Ca^{2+} and Mg^{2+}, and a dissociation constant (K_d) of <1 nM. We have also demonstrated that the ZP sensors undergo effective two-photon excitation. ZP3 has been utilized for imaging endogenous pools of ionic Zn^{2+} in live hippocampal slices with TPM. Finally, we note that the difluorofluorescein monocarboxaldehyde building block should find utility for accessing future candidates for metal ion sensing.

Acknowledgment. This work was supported by a grant to S.J.L. from the National Institute of General Medical Sciences (GM 65519). C.J.C. acknowledges the Jane Coffin Childs Foundation for a postdoctoral fellowship. E.M.N. thanks the NDSEG for a graduate fellowship. M.S. is an Investigator at the Howard Hughes Medical Institute. The MIT Department of Chemistry Instrument Facility is funded through the National Science Foundation (CHE-9808061, CHE-9808063, and DBI-9729592).

IC049293D